Atomic structure and energy of the {113} planar interstitial defects in Si

Masanori Kohyama
Glass and Ceramic Material Department, Government Industrial Research Institute, Osaka, 1-8-31 Midorigaoka, Ikeda, Osaka 563, Japan

Seiji Takeda
Department of Physics, College of General Education, Osaka University, Toyonaka, Osaka 560, Japan
(Received 13 July 1992)

The atomic structure and energy of the {113} planar interstitial defects in Si have been examined by energy-minimization calculations using the Stillinger-Weber potential, based on the atomic model recently proposed by Takeda from the high-resolution transmission electron microscopy image. The atomic model contains no dangling bonds and consists of the two kinds of structural units characterized by an interstitial atom chain along the ⟨110⟩ direction and by an eight-membered ring. It has been shown from the calculations that the atomic models, in which the arrangement and composition of the two kinds of structural units are similar to the observed structure, can exist stably with relatively small bond-length and bond-angle distortions, and with much smaller energy per interstitial atom than that of the isolated self-interstitial in bulk Si. Through the calculations of models with various composition or arrangement of the structural units, we have elucidated the stability of the eight-membered rings, the mechanism of generation of the {113} defects, the origin of the observed arrangement of the two kinds of structural units, and the mechanism of unfaulting of the {113} defects. It can be said that the {113} planar defects are formed by the sequential generation of the structural units containing the interstitial atom chain side by side on the {113} plane, and the structural units containing the eight-membered ring are inserted separately so as to relax the strain energy of the sequence of the structural units. The unfaulting is the transformation of the sequence of the structural units into the perfect crystal containing additional two net {113} atomic layers under the simultaneous rigid-body translation. It is possible to explain the structure and properties of the {113} planar defects in Si from the viewpoint of the arrangement of the structural units containing no dangling bonds similar to the case of the ⟨110⟩ symmetrical tilt grain boundaries in Si, and without any direct effects of impurities. This is originated from the general nature of covalent crystals which demands that all the atoms are four coordinated.

I. INTRODUCTION

The {113} planar defects or rodlike defects are well known as peculiar defects generated by electron or ion irradiation only in Si or Ge.[1–3] Under the subsequent irradiation, the defects often exhibit unfaulting into perfect dislocation loops of interstitial-type on the {113} plane without leaving any visible precipitates. Thus it is possible that the {113} defects are extended defects of self-interstitial atoms on the {113} plane like a Frank-type loop on the {111} lane. However, there have been no reports on the aggregation of point defects on the {113} plane in other materials. Therefore it is very interesting to elucidate the atomic structure and the mechanism of generation of the {113} planar defects. For this purpose, a lot of experimental studies have been performed, and various atomic models of the {113} defects have been proposed.[2–7] However, there have been no conclusive models.

Recently, Takeda has carried out a high-resolution transmission electron microscopy (HRTEM) observation of the {113} planar defects with ⟨110⟩ incidence in Si, and constructed a new atomic model from the cross-sectional HRTEM image.[8] The atomic model reveals a new kind of lattice reconstruction involving self-interstitials in the interior of a Si crystal, and is described by arrangement of two kinds of structural units on the {113} plane. These structural units consist of atomic rings without any dangling bonds in the ⟨110⟩ projection. One kind of unit is characterized by an eight-membered ring, and another kind of unit contains a self-interstitial atom chain along the ⟨110⟩ direction, which constitutes a tiny rod of hexagonal Si. It has been also found that the two kinds of structural units are arranged on the {113} plane without any long-range periodicity along the ⟨332⟩ direction, although there exist some short-range order along the ⟨332⟩ direction and the periodicity along the ⟨110⟩ direction. This observation is in good agreement with the observed electron diffraction.[9] Recently, it has been shown that the {113} planar defects in Ge have isomorphic structure.[10]

It should be noted that the present atomic model of the {113} planar defects has many features in common with the atomic models of the ⟨110⟩ symmetrical tilt grain boundaries in Si or Ge.[11] Both structures are constructed by arranging structural units consisting of atomic rings in the ⟨110⟩ projection without any dangling bonds, and have periodicity along the ⟨110⟩ direction. A lot of observations[12,13] and theoretical calculations[14–18] have shown that several such models of the ⟨110⟩ symmetri-

cal tilt boundaries in Si or Ge can exist stably. However, eight-membered rings such as those in the present atomic model of the {113} defects have never been observed in grain boundaries in Si or Ge.

Now, it is of much importance to examine the stability of the present atomic model of the {113} planar defects through theoretical calculations of energies and relaxed configurations. In this paper we perform energy-minimization calculations of the atomic model of the {113} planar defects using the Stillinger-Weber (SW) potential.[19] The calculated results are compared with those of the ⟨110⟩ symmetrical tilt grain boundaries in Si. And through calculations of various models with various composition or arrangement of the structural units, we investigate the stability of the eight-membered rings, the origin of the observed arrangement of the structural units in the {113} defects, and the mechanism of generation and unfaulting of the {113} defects.

II. POTENTIAL

For calculations of energies and relaxed configurations of the atomic models, we have used the SW potential.[19] This is an empirical two- and three-body potential between atoms for solid or liquid Si. The two-body part includes a bond-stretching component, and the three-body part includes both bond-stretching and bond-bending components. The potential energy Φ of the system, which is the total energy without the kinetic energy of atoms, can be expressed by the SW potential as follows:

$$\Phi=\frac{1}{2}\sum_i\sum_{j\neq i}\varepsilon f_2(r_{ij}/\sigma)+\sum_i\sum_{\substack{j,k\neq i\\ j<k}}\varepsilon h(r_{ij}/\sigma,r_{ik}/\sigma,\theta_{jik})\ , \tag{1}$$

where

$$f_2(r_{ij}/\sigma)=\begin{cases}A\,[B(r_{ij}/\sigma)^{-4}-1]\exp\{[(r_{ij}/\sigma)-1.80]^{-1}\}\ , & r_{ij}<1.80\sigma\\ 0\ , & r_{ij}\geq 1.80\sigma\ ,\end{cases} \tag{2}$$

and

$$\begin{aligned}h(r_{ij}/\sigma,r_{ik}/\sigma,\theta_{jik})=&\lambda\exp\{\gamma[(r_{ij}/\sigma)-1.80]^{-1}\}\\ &\times\exp\{\gamma[(r_{ik}/\sigma)-1.80]^{-1}\}\\ &\times(\cos\theta_{jik}+\tfrac{1}{3})^2\ .\end{aligned} \tag{3}$$

The two-body function f_2 sharply increases at short distances, has a minimum when r_{ij} is the first-neighbor distance of bulk Si, and vanishes smoothly with r_{ij} beyond $1.80\sigma=0.694a_0$ (a_0 is the lattice constant), which is less than the second-neighbor distance of bulk Si. Thus the sum of the first term in Eq. (1) includes only the neighbor j within the cutoff distance 1.80σ from the respective atom i. The three-body function h is nonzero only when both r_{ij} and r_{ik} are shorter than the cutoff distance 1.80σ. Thus the sum of the second term in Eq. (1) includes possible pairs of the neighbors within the cutoff distance from the respective atom i. θ_{jik} is the angle between the two vectors $\mathbf{r}_{ij}$ and $\mathbf{r}_{ik}$. The bond-bending effect is included through the form of $(\cos\theta_{jik}+\frac{1}{3})^2$, which is zero for the ideal tetrahedral angle of bulk Si.

In the SW potential, it is possible to express the atomic forces analytically as well as the potential energy by differentiating the potential function. All the parameters in the potential, A, B, γ, ε, λ, σ, and the cutoff parameter 1.80, have been determined so as to ensure that the diamond structure is energetically most stable, and that the calculated melting points and liquid-structure factors agree with experimental results. In the present study, we have used the original values of the parameters determined by Stillinger and Weber,[19] although only the value of σ has been readjusted so as to reproduce the correct lattice constant in the computer. The difference in σ from the original value is a slight decrease of about 0.000 04 nm.

The SW potential has been used with considerable success in studies of various properties of the crystalline, amorphous, and liquid Si.[20,21] The SW potential has also been used extensively in studies of atomic structures and energies of lattice defects in Si such as point defects,[22] dislocations,[23] and grain boundaries.[24,25] The advantages of the SW potential are that the range of applicability is not limited to four-coordinated structures, and that energies and atomic forces are easily obtained with relatively short computing time even for systems containing hundreds of atoms, which enable us to perform molecular dynamics or energy-minimization calculations of complicated structures.

A weak point of the SW potential is that there are no guarantees that the determined potential function and parameters can be applicable for any local environment. This seems to be serious for structures containing atoms whose coordinations are significantly different from the ideal-crystal value of four, such as surfaces[26] or clusters,[27,28] and various types of new model potentials beyond pair potentials other than the SW potential have been developed so as to improve the applicability and reliability.[29,30] However, in the present study, we deal with the atomic models where all the atoms are four coordinated. Thus we think that the present results by the SW potential are reliable at least qualitatively.

Another shortcoming of the SW potential is that the energy difference between diamond Si and hexagonal Si is regarded as being zero. This might cause some uncertainty in the calculated energies of the structures containing rods of hexagonal Si in the present models. However, the energy difference between the two crystal structures is small, which is estimated to be about 0.01 eV/atom by the first-principles calculations,[31] and we think that the omission of this effect should have no serious effect on the present results.

III. ATOMIC MODELS AND COMPUTATIONAL PROCEDURE

Figure 1(a) shows the ⟨110⟩ projection of the two kinds of structural units constituting the model of the {113} planar interstitial defects in Si proposed by Takeda.[8] One unit contains a self-interstitial atom chain along the ⟨110⟩ direction,[4] which belongs to a pair of six-membered rings corresponding to a tiny rod of hexagonal Si,[3] surrounded by seven- and five-membered rings. Another unit contains an eight-membered ring surrounded by five- and six-membered rings. The former and the latter units are called an *I* unit and an *O* unit, respectively, in the present paper. Each unit has the width of $[-3,-3,2]a_0/4$ along the ⟨332⟩ direction, and repeats periodically along the ⟨110⟩ direction. The *I* unit is constructed by inserting the interstitial atom chain in the *O* unit. It should be noted that the *O* unit has no self-interstitials or vacancies, and the *I* unit contains two interstitial atoms per period along the ⟨110⟩ direction.

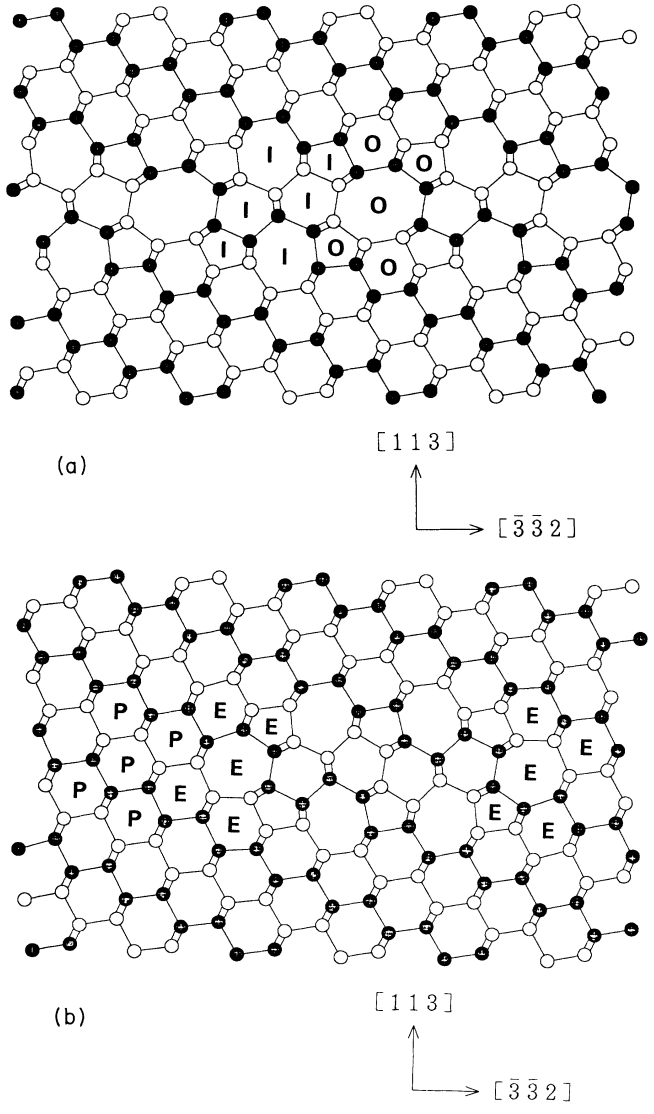

FIG. 1. The ⟨110⟩ projection of the structural units constituting the {113} defects in Si. (a) *I* and *O* units. (b) *E* and *P* units. Atomic rings constituting the respective units are indicated by the symbols of the units. The open and closed circles indicate the atoms of the two different atomic heights along the ⟨110⟩ direction.

Two other kinds of structural units on the {113} plane can also be defined as shown in Fig. 1(b). The *E* units constitute the edges of the {113} planar defects, namely, the edges of the sequence of the *I* or *O* units along the {332} direction, as shown in Ref. 32. And the *P* unit constitutes the perfect crystal. All these units also have the same width along the ⟨332⟩ direction.

It is possible to construct various models of the {113} planar or rodlike defects without any dangling bonds by arranging these four kinds of structural units on the {113} plane. The cross-sectional HRTEM image[8] can be interpreted as the sequence of the *I* and *O* units such as "*IOIOIOIIOIOIIOIIIO* . . .," where the ratio of the *I* units to the sum of all the units is 62%, and there exists no obvious long-range periodicity in the arrangement of the units. However, there exists some short-range order. For example, *O* units are arranged separately at intervals of one or two *I* units, occasionally three *I* units. In Ge, an observed HRTEM image can also be interpreted as a similar arrangement of the structural units, and the ratio of the *I* units is 65%.[10]

In the present paper, for computational convenience, we have dealt with only the models with the periodicity along the ⟨332⟩ direction as well as the ⟨110⟩ direction. For example, Fig. 1(a) shows the $|IO|$ model where the *I* and *O* units repeat periodically along the ⟨332⟩ direction. In the present paper, the symbols of the units sandwiched by "|" represent the arrangement of the units constituting one period along the ⟨332⟩ direction in the periodic models. We think that it is possible to investigate the stability of observed local structure or short-range order by calculations of such models with periodicity along the ⟨332⟩ direction.

Energy minimization has been performed by iterative relaxations of the atomic positions according to atomic forces in the SW potential. Atoms in the region of the width of about 3.3 nm on both sides of the planar defect between the fixed bulk crystals have been relaxed under the periodic boundary condition along the ⟨332⟩ and ⟨110⟩ directions. Iterations have been terminated when all the atomic forces are less than 0.01 eV/Å.

In the starting configuration before relaxations, the two bulk crystals are set at the positions with a given rigid-body translation, and atomic positions of several {113} atomic layers at the core of the planar defect are given by hand properly. The rigid-body translation between the two crystals is defined as compared with the perfect crystal structure containing no defects. In the present paper, the translation means the shift of the upper crystal against the lower crystal shown in Fig. 1, and is expressed in the coordinates of Fig. 1. The estimated translation from the HRTEM image is $0.032a_0[116]$.[8] This value is close to that determined in the diffraction imaging technique.[1] The observed translation can be decomposed into the two components parallel and normal to the {113} plane as $0.096a_0[-3,-3,2]/$

$11+0.64a_0[113]/11$. Calculations have been performed under the observed translation, and also the most favorable translations have been determined for respective models by iterative energy minimization.

IV. RESULTS AND DISCUSSION

A. Calculated models and results

We have dealt with models with various compositions or arrangements of the four kinds of structural units. Models are constructed by increasing the density of the aggregated interstitial atoms, namely the I units, from 0% to 100%. We have dealt with the models up to those with fivefold periodicity along the $\langle 332 \rangle$ direction. Table I shows the calculated results of the models under the most favorable rigid-body translations, respectively. Table II shows the results of the models with the density of the I units equal or larger than 50% under the observed rigid-body translation. In Tables I and II, the models indicated by an asterisk are those of which at least one period of the sequence of the structural units along the $\langle 332 \rangle$ direction has been observed as local structure of the $\{113\}$ planar defects.[8]

There exist several rules in the construction of models. For example, the E units must exist at the edges of the sequence of the I or O units, and either side of the E unit must be connected to the E or P units. Thus the E unit cannot exist solely between the I units, differently from the O units. The sequence of the two E units can be transformed into the sequence of the two O units by changing the bond topology. Of course, the present models do not include all the possible arrangements. However, we think that the main important models have been dealt with in order to accomplish the purposes of the present paper as will be shown in Secs. IV B–IV F.

In Tables I and II, total energies per unit cell, interfacial energies, and energies per aggregated interstitial atom are listed as well as the ranges of the bond-length and bond-angle distortions in the relaxed configurations. The total energy values are defined as compared with the perfect crystal of the same number of atoms. The interfacial energy is the total energy divided by the area of the interface. The energy per aggregated interstitial atom is obtained by dividing the total energy per unit cell by the number of aggregated interstitial atoms in the unit cell.

It should be noted that the comparison between the total energies or interfacial energies of the models containing different numbers or densities of the aggregated interstitial atoms is rather meaningless. The total energy values per unit cell should be compared with each other after making equal the total numbers of aggregated or isolated interstitial atoms between the models, for example, by adding the energy of isolated self-interstitials in bulk Si. The energy per aggregated interstitial atom should be the most proper measure for judging the relative stability between the models as the structure of aggregation of self-interstitials from the starting point of the bulk crystal saturated with isolated self-interstitials generated by electron or ion irradiation. Table III lists the energies per aggregated interstitial atom of the main stable structures for respective densities of the I units within the present models.

In Tables I and II the differences between the results for the two types of the rigid-body translations are small qualitatively, although the energies are slightly larger in Table II. In Table I the favorable translations of respective models are generally a dilatation along the $\langle 113 \rangle$ direction coupled with a shift parallel to the $\langle 332 \rangle$ direction similar to the observed translation, although the highly hypothetical $|O|$ model has a peculiar translation. The magnitude of the favorable translation generally increases as the density of the I units increases, because the translations are caused by the aggregated interstitial atoms. Of course, the favorable translations depend on not only the density of the I units but also the arrangement of the units or the kinds of the units other than the I units. The $|I|$ model contains the highest density of the aggregated interstitial atoms, where a dilatation along the $\langle 113 \rangle$ direction is largest and reaches nearly the width of two net $\{113\}$ atomic layers, $a_0/\sqrt{11}$. This type of structure containing two net $\{113\}$ atomic layers is connected with the unfaulting as will be discussed in Sec. IV F.

It should be noted that the present calculated structures are planar defects with infinite two-dimensional periodicity, or infinite periodic arrays of rodlike defects. This feature is different from the observed $\{113\}$ defects with finite sizes. It can be said that the size of the defect should influence the value of the rigid-body translation, and the observed and calculated optimum values of translations must be interpreted by considering this point as discussed in Sec. IV B.

As shown in Table III, it should be emphasized that the energies per aggregated interstitial atom in all the present models are much less than the energy accompanied with one isolated interstitial atom in bulk Si, which is the formation energy of a self-interstitial and is estimated to be 5 or 6 eV in the calculations using the SW potential[22] or the first-principles density-functional theory.[33] This indicates the possible energy gains in the generation of the present atomic structures from the bulk crystal saturated with isolated self-interstitials. This is because all the atoms can be four-coordinated in the present models differently from isolated self-interstitials in bulk Si. The detailed analyses of the calculated results and the discussion are given in Secs. IV B–IV F.

B. Stability of the $|IO|$, $|IOIIO|$, $|IIO|$, and $|IIIO|$ models

Within the present models, the $|IO|$, $|IOIIO|$, $|IIO|$, and $|IIIO|$ models relatively well resemble the observed structure,[8] where O units are arranged separately at intervals of one or two I units, occasionally three I units, without any long-range periodicity, and the density of the I units is 62%. These models can be regarded as local structures constituting the observed structure.

The calculated results of these models in Tables I and II are qualitatively similar to each other. It has been shown that these models have stable configurations with local energy minima within the topology of the models under both types of rigid-body translations. The comparison between the simulated images of the relaxed

TABLE I. Summary of calculated results under the optimum rigid-body translations for respective models. R_I is the ratio of the I units in the model. T is the calculated optimum translation. This is expressed by being decomposed into the two components along the $[-3,-3,2]$ direction parallel to the $\{113\}$ plane and along the $[113]$ direction normal to the $\{113\}$ plane. These components are listed in this order in the parentheses in the unit of the width of two $\{113\}$ atomic layers, $a_0/\sqrt{11}$. The observed translation (Ref. 8) is (0.14, 0.64) in the present expression. E_{tot}, E_{if}, and E_{is} are the total energy per unit cell, the interfacial energy, and the energy per aggregated interstitial atom. Δr and $\Delta\theta$ indicate the ranges of the bond-length and bond-angle distortions of the relaxed configurations, respectively. The asterisks indicate the models of which at least one period of the sequence of the structural units has been observed as local structure of the $\{113\}$ planar defects (Ref. 8).

R_I (%)	Model	T ($a_0/\sqrt{11}$)	E_{tot} (eV/cell)	E_{if} (J/m^2)	E_{is} (eV)	Δr	$\Delta\theta$
0	$\|O\|$	(−0.22,0.49)	2.71	1.777		−0.2% to 11.1%	−20.7° to 41.8°
20	$\|PEIEP\|$	(0.05,0.29)	3.21	0.420	1.60	−2.9% to 2.1%	−19.0° to 18.9°
25	$\|EIEP\|$	(0.06,0.36)	3.13	0.513	1.57	−2.7% to 2.3%	−19.2° to 18.7°
33	$\|EIE\|$	(0.09,0.48)	3.00	0.655	1.50	−2.4% to 3.0%	−19.5° to 18.7°
	$\|IOO\|$	(0.14,0.71)	4.57	0.998	2.29	−1.1% to 6.7%	−18.9° to 33.3°
40	$\|EIIEP\|$	(0.10,0.47)	4.65	0.609	1.16	−2.5% to 2.6%	−21.2° to 22.6°
50	$\|EIIE\|$	(0.13,0.59)	4.41	0.722	1.10	−2.3% to 3.3%	−21.5° to 22.4°
	$\|IIOO\|$	(0.14,0.77)	5.39	0.884	1.35	−2.1% to 5.3%	−21.7° to 30.6°
	$\|IO\|$*	(0.17,0.78)	2.23	0.731	1.12	−1.1% to 2.8%	−19.0° to 22.0°
60	$\|IOIIO\|$*	(0.21,0.81)	5.58	0.732	0.93	−1.8% to 2.0%	−21.2° to 22.1°
66	$\|IIO\|$*	(0.22,0.83)	3.41	0.745	0.85	−1.7% to 2.2%	−21.1° to 22.0°
75	$\|IIIO\|$*	(0.23,0.85)	4.98	0.816	0.83	−1.7% to 2.6%	−21.8° to 24.3°
80	$\|IIIIO\|$	(0.23,0.87)	6.69	0.876	0.84	−1.8% to 2.7%	−22.0° to 24.6°
100	$\|I\|$	(0.25,0.92)	1.73	1.135	0.87	−2.2% to 1.7%	−19.3° to 22.4°

TABLE II. Summary of calculated results under the observed rigid-body translation, $0.032a_0[116]$, which corresponds to (0.14,0.64) in the expression in Table I.

R_I (%)	Model	E_{tot} (eV/cell)	E_{if} (J/m^2)	E_{is} (eV)	Δr	$\Delta\theta$
50	$\|EIIE\|$	4.42	0.724	1.10	−2.2% to 3.5%	−21.6° to 22.4°
	$\|IIOO\|$	5.46	0.894	1.37	−2.4% to 5.0%	−21.6° to 31.0°
	$\|IO\|$*	2.26	0.742	1.13	−1.4% to 2.6%	−18.8° to 22.4°
60	$\|EIIIE\|$	6.06	0.794	1.01	−2.4% to 3.5%	−22.2° to 24.4°
	$\|IIIOO\|$	6.90	0.904	1.15	−2.1% to 4.6%	−22.4° to 30.2°
	$\|IOIIO\|$*	5.72	0.749	0.95	−2.2% to 1.6%	−20.8° to 22.4°
66	$\|IIO\|$*	3.51	0.767	0.88	−2.1% to 1.7%	−20.6° to 22.4°
75	$\|IIIO\|$*	5.16	0.845	0.86	−2.1% to 1.9%	−21.3° to 24.8°
80	$\|IIIIO\|$	6.93	0.909	0.87	−2.1% to 2.0%	−21.4° to 25.2°
100	$\|I\|$	1.81	1.185	0.90	−2.5% to 1.0%	−18.6° to 22.9°

configurations of these models and the observed HRTEM images is now being performed. The bond-angle and bond-length distortions in the relaxed configurations of these models are relatively small within all the calculated models. The absolute values of the bond-length distortions do not exceed 3%, and those of the bond-angle distortions do not exceed 25°. These ranges are similar to those in the previous theoretical calculations of symmetrical tilt grain boundaries in Si.[14−18] This indicates the possible existence of the present models as local structures of the {113} planar defects in Si.

For more precise comparison, we have carried out similar calculations of the {221} $\Sigma=9$ boundary, which is a typical ⟨110⟩ symmetrical tilt grain boundary in Si. We have dealt with the atomic model consisting of zigzag arrangement of five- and seven-membered rings, of which the stability has already been examined experimentally and theoretically.[12−15,18] Atoms in the region of the width of 3.3 nm on both sides of the interface are relaxed in the same way. The calculated interfacial energy is 0.454 J/m^2, which is in good agreement with the value by Phillpot and Wolf[24] using the same method. The optimum rigid-body translation is a dilatation of 0.013 nm normal to the interface, and the bond-length and bond-angle distortions range from −1.5% to +1.9%, and from −16.3° to +21.1°, respectively. These results are consistent with the previous theoretical results of this boundary in Si through electronic structure calculations,[14,15,18] although the energy is somewhat overestimated as compared with the previous results, which should be a drawback peculiar to the SW potential.

It can be said that the range of the bond distortions in the $|IO|$, $|IOIIO|$, $|IIO|$, and $|IIIO|$ models is similar to that in the {221} $\Sigma=9$ boundary in Si. However, the maximum values of the bond distortions in these models are somewhat larger than those in the {221} $\Sigma=9$ boundary, and the calculated interfacial energies of these models are about 1.6 to 1.9 times larger than that of the {221} $\Sigma=9$ boundary. It can be said that a relatively high density of strain energy is contained in the present models of the {113} defects as compared with the {221} $\Sigma=9$ boundary or other ⟨110⟩ symmetrical tilt grain boundaries in Si. This should be concerned with the nature of quasistability of the {113} defects that these defects are generated only under special conditions and are transformed and unfaulted frequently.[1−3]

The energies per aggregated interstitial atom of the $|IO|$, $|IOIIO|$, $|IIO|$, and $|IIIO|$ models are about 0.8 to 1.1 eV as shown in Table III, and much smaller than the energy accompanied with an isolated self-interstitial atom in bulk Si, which is estimated to be 5 or 6 eV as mentioned above. This also supports the possible existence of the present structures.

About the rigid-body translations, it should be noted that the most favorable ones for the $|IO|$, $|IOIIO|$, $|IIO|$, and $|IIIO|$ models are qualitatively similar to the observed one[8] as shown in Table I, which also supports the possible existence of these structures. However, the calculated optimum values are slightly larger than the observed one in both the ⟨332⟩ and ⟨113⟩ directions. We think that this difference might be caused by the finite sizes of the real planar defects as mentioned above, besides possible errors in the present theoretical method or the experimental observation. The finite sizes of the defects should cause some suppression of the rigid-body translation in the bulk crystal as compared with the calculated structures with infinite two-dimensional extent.

About the $|IOIIO|$ model, we have found that this structure is most stable as compared with other possible

TABLE III. Summary of calculated energies per aggregated interstitial atom of main stable models for respective densities of the I units under the two types of the rigid-body translations.

R_I (%)	Model	E_{is} under the optimum translation (eV)	E_{is} under the observed translation (eV)
20	$\|PEIEP\|$	1.60	
25	$\|EIEP\|$	1.57	
33	$\|EIE\|$	1.50	
40	$\|EIIEP\|$	1.16	
50	$\|EIIE\|$	1.10	1.10
	$\|IO\|$*	1.12	1.13
60	$\|IOIIO\|$*	0.93	0.95
66	$\|IIO\|$*	0.85	0.88
75	$\|IIIO\|$*	0.83	0.86
80	$\|IIIIO\|$	0.84	0.87
100	$\|I\|$	0.87	0.90

models containing the same density of the *I* units, such as the |*IIIOO*| and |*EIIIE*| models, as shown in Table II. There exist relatively large bond-length and bond-angle distortions especially in the |*IIIOO*| model. The present result is in good agreement with the HRTEM observations, where the arrangement of the units similar to the |*IIIOO*| model has never been found in Si or Ge.[8,10,32]

C. Stability of the eight-membered rings

Here, we analyze the stability of the eight-membered rings, namely, the *O* units. As shown in Table I, the |*O*| model consisting of the sequence of the eight-membered rings on the {113} plane has a stable configuration with a local energy minimum under a peculiar translation. However, this structure contains large bond-length and bond-angle distortions as much as +11.1% and +41.8°, and high strain energies. It can be concluded that this structure should be unstable in the bulk crystal and should be easily transformed into the perfect crystal by shifting the crystals and changing the bond topology.

As shown in Tables I and II, the structure containing the *O* units is not the most stable one for the respective densities of the *I* units less than or equal to 50%. For example, the |*EIE*| model is more stable than the |*IOO*| model. And the |*EIIE*| model is more stable than the |*IIOO*| and |*IO*| models, although the energy difference per aggregated interstitial atom between the |*IO*| model and the |*EIIE*| model is very small. On the other hand, for the models in which the density of the *I* units exceeds 50%, the structure containing the *O* units can be the most stable one as in the case of the |*IOIIO*| model.

It can be said that the *O* units (or the eight-membered rings) are stabilized by being sandwiched separately between the *I* units. This point can be seen clearly in comparison between the |*IO*| and |*IIOO*| models and between the |*IOIIO*| and |*IIIOO*| models in Tables I and II. The structures of the |*IO*| and |*IOIIO*| models, where the *O* units are sandwiched separately between the *I* units, are much more stable than the structures of the |*IIOO*| and |*IIIOO*| models, respectively, where the *O* units are adjacent to each other, in spite of the same densities of the *I* units. There exist relatively larger bond-length and bond-angle distortions associated with the eight-membered rings in the |*IIOO*| and |*IIIOO*| models as observed in the |*O*| model. The absolute values of the bond distortions in these models reach as much as 5% and 30°, although those in the |*IO*| and |*IOIIO*| models do not exceed 3% and 23°.

Figure 2 shows the relaxed configurations and the strain energies of respective atoms of the |*IO*| and |*IIOO*| models under the most favorable translations. The energies of respective atoms can be obtained by partitioning the energy terms in the SW potential into the respective bonds and bond angles as shown in Eq. (1), and reflect local distortions. It is obvious that the eight-membered rings contain relatively large bond distortions and strain energies in the |*IIOO*| model as compared with the |*IO*| model.

The present result that the *O* units or the eight-membered rings can be stabilized by being sandwiched separately between the *I* units is in good agreement with the HRTEM observations,[8,10,32] where all the *O* units are arranged separately between the *I* units and no *O* units neighboring side by side have been observed. In addition, the present results mean that the density of the *O* units does not exceed 50% in the sequence of the structural units, which is also in good agreement with the observations.

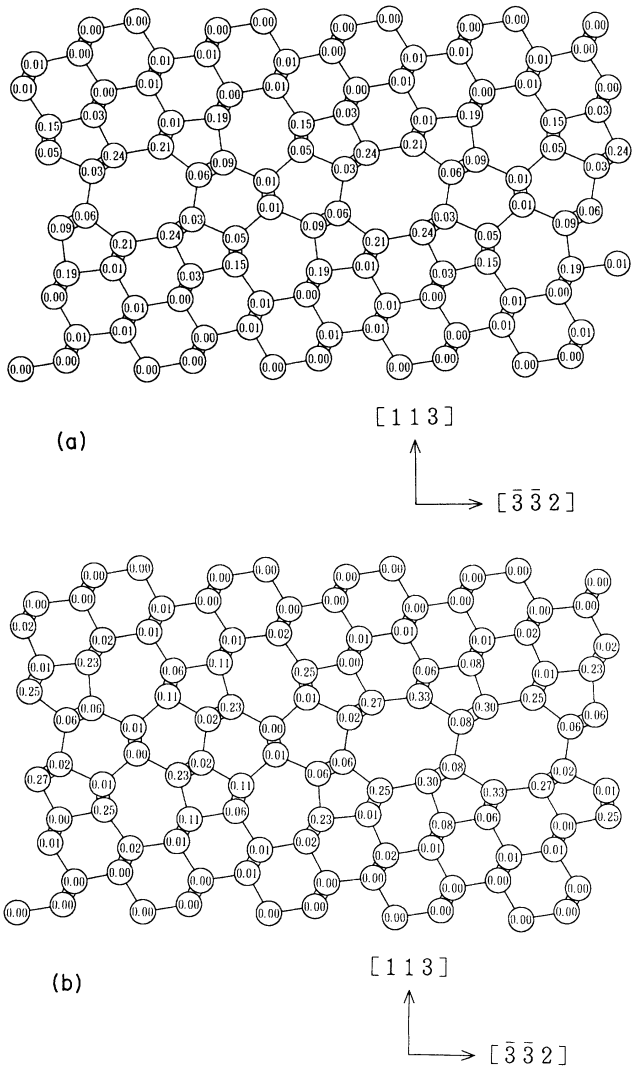

FIG. 2. The relaxed configurations and the strain energies of respective atoms of the |*IO*| model (a) and of the |*IIOO*| model (b) in Si under the optimum rigid-body translations.

D. Mechanism of generation of the {113} planar defects

About the mechanism of generation of the {113} planar defects, we think that the first stage is the formation of the *I* unit in the bulk crystal, in other words, the formation of a rodlike defect containing an interstitial atom chain, under the condition of a lot of isolated self-interstials. As discussed in Ref. 32, this rodlike defect can be described as "*EIE*" by using the present structural units. From the present results of the |*PEIEP*| model

shown in Table I and Fig. 3, it can be said that such atomic structure of the rodlike defect can exist stably with relatively small bond-length and bond-angle distortions and that the energy gain can be expected in the formation of such rodlike defects from isolated self-interstitials.

The second stage is probably the formation of neighboring I units such as the process from "*EIE*" to "*EIIE*." We think that the rodlike defects grow into the $\{113\}$ planar defects by such sequential generation of the I units side by side along the $\langle 332 \rangle$ direction on the $\{113\}$ plane.

About this point, the present calculations have shown that there exist energy gains in the I units neighboring side by side on the $\{113\}$ plane as compared with the isolated I units. For example, in the results of the $|PEIEP|$ and $|EIIEP|$ models shown in Table I, the energy per aggregated interstitial atom in the latter model is smaller than that in the former model. This indicates the energy gain in the formation of the defect described as "*EIIE*" as compared with two sets of the defects described as "*EIE*."

In detail, in the $|PEIEP|$ model, the sum of the strain energies of 16 atoms at the I unit enclosed by a dashed line in Fig. 3 is 1.12 eV, and the sum of those of 16 atoms at the E units on both sides of the I unit enclosed similarly in Fig. 3 is 1.32 eV. In the $|EIIEP|$ model, the similar sums for the two I units are 1.21 and 1.21 eV, and the similar sum for the E units is 1.30 eV. A greater part of the strain energy is concentrated at the core region of the structural units in both the structures. Although the strain energy is slightly increased in the I units neighboring side by side in the $|EIIEP|$ model, the total energy per I unit or per interstitial atom can be reduced in the $|EIIEP|$ model as compared with the $|PEIEP|$ model because of the reduction of the number of E units per I unit. Similar results can be obtained in the comparison between the $|EIE|$, $|EIIE|$, and $|EIIIE|$ models, although neighboring arrays of rodlike defects are very close on the $\{113\}$ plane in these models.

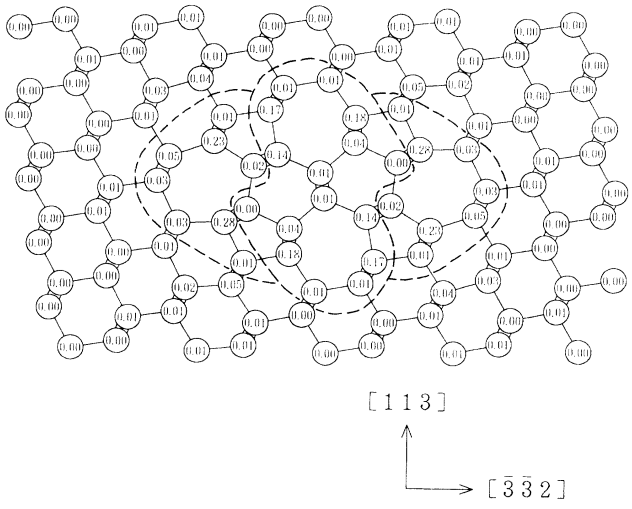

FIG. 3. The relaxed configuration and the strain energies of respective atoms of the $|PEIEP|$ model in Si under the optimum rigid-body translation. Dashed lines enclose the atoms of which the strain energies are included in the sum of the strain energies of the core region of a respective unit.

Generally, all the isolated I units induce E units and related distortions on both sides, respectively. On the other hand, the I units neighboring side by side on the $\{113\}$ plane generate such E units and distortions only at the edges of the sequence of the I units, which causes reduction of the total energy per I unit or per interstitial atom. This should promote the growth of the sequence of I units on the $\{113\}$ plane rather than the generation of isolated I units.

The present discussion of the mechanism of the generation of the $\{113\}$ defects is consistent with many observations, where elongated defects along the $\langle 110 \rangle$ axis are generated initially and then defects tend to widen into planar defects.[1] Of course, the sites of nucleation and the growth rate should be influenced by the environment in the crystal, such as the stress distribution caused by other defects or impurities. As discussed in Ref. 32, the steps in the $\{113\}$ defects and related complicated structures should be caused by such effects.

The present discussion about the generation of the $\{113\}$ defects does not include any direct effects of impurities. Of course, there have been experimental results indicating the effects of impurities such as carbon in the generation of the $\{113\}$ defects.[34] It might be possible that impurities are connected with the nucleation of the I unit itself or the growth of the I unit, although the structure of the $\{113\}$ defects itself can be explained without any effects of impurities.

E. Origin of the observed arrangement of the *I* and *O* units

As shown above, the mechanism of the generation of the $\{113\}$ planar defects can be explained by the nucleation of the rodlike defects and the growth to the planar defects through generation of the I units side by side on the $\{113\}$ plane along the $\langle 332 \rangle$ direction. However, the observed structure contains not only the I units but also the O units. The reason why the O units are contained in the observed structures and the origin of the stability of the observed arrangement of the two kinds of structural units can be deduced from the present calculations as follows.

About the results of the models containing only the I and O units from the $|IO|$ model to the $|I|$ model shown in Table III, the energy per aggregated interstitial atom initially decreases as the density of the I units increases. Then the energy has a minimum at the $|IIIO|$ model, and increases toward the $|I|$ model. This trend is consistent with the observed structure, although the observed density of the I units is 62% in Si.

The reason for the above behavior of the energy per interstitial atom in the models consisting of the I and O units can be explained by the following two effects. First, the increase of the density of the I units means the decrease of the number of O units per I unit, which causes the decrease of the energy per aggregated interstitial atom, similarly to the case of the reduction of the number

of E units per I unit by the sequential generation of the I units side by side on the {113} plane discussed in Sec. IV D. Second, on the other hand, the increase of the density of the I units causes the increase of the strain energy at the I units themselves. These two conflicting effects dominate the above behavior of the energy per aggregated interstitial atom. In other words, the O units inserted properly between the sequence of the I units act so as to relax the strain energy at the I units, and the most favorable structure can be accomplished.

This point can be seen clearly by analyzing the strain energies of respective atoms. Figure 4 shows the relaxed configuration and the strain energies of respective atoms of the $|IIO|$ model. The sums of the strain energies of 16 atoms at the I unit in the $|IIO|$ model enclosed by dashed lines in Fig. 4 are 1.17 and 1.17 eV, and that of 14 atoms at the O unit enclosed similarly is 1.02 eV. In the $|IIIO|$ model, the similar sums for the I units are 1.31, 1.26, and 1.31 eV, and that for the O unit is 0.98 eV. In the $|IIIIO|$ model, those for the I units are 1.34, 1.42, 1.42, and 1.34 eV, and that for the O unit is 1.00 eV. In the $|I|$ model, that for the I unit is 1.72 eV. All these results are those under the optimum rigid-body translations, and a greater part of the strain energy is concentrated at the core region of the structural units in all the structures. It is clear that the strain energy at the I units increases as the sequence of the I units becomes more dense from the $|IO|$ model to the $|I|$ model, and this effect counterbalances the energy gain by reduction of the density of the O units. And in other words, the O units are inserted so as to relax the strain energy of the sequence of the I units.

This is the reason of the present result that the $|IIIO|$ model has the least energy per aggregated interstitial atom. And this can well explain the arrangement of the I and O units in the HRTEM observation.[8] It can be said that the reason why the interstitial atoms are aggregated on the {113} plane in Si or Ge is the sequential generation of the I units side by side on the {113} plane and the stabilization by introducing the O units.

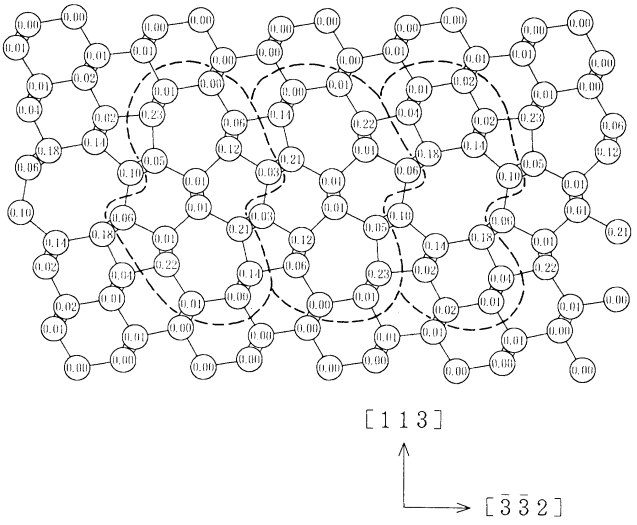

FIG. 4. The relaxed configuration and the strain energies of respective atoms of the $|IIO|$ model in Si under the optimum rigid-body translation. Dashed lines enclose the atoms of which the strain energies are included in the sum of the strain energies of the core region of a respective unit.

However, some problems still remain. The observed ratio of the I units is 62%, and the $|IOIIO|$ or $|IIO|$ models more resemble the observed structure than the calculated most favorable $|IIIO|$ model, although the difference in the calculated energy per interstitial atom is small between these models. And there is no long-range periodicity along the ⟨332⟩ direction in the observed arrangement. We think that these problems might be explained by the effects of configurational or vibrational entropy and finite temperature. Otherwise, there might exist the effect of the sizes of the defects, or the effect of the kinetics in nucleation and growth of the defects. The eight-membered rings seem to be connected with atomic diffusion in growth of the defects. All these effects have not been included in the present calculations. Of course, there is the uncertainty caused by the present theoretical method using empirical potential. However, it should be emphasized that the present calculations have successfully reproduced the trends of the observed structure, and we have shown the main origin of the observed arrangement of the structural units.

F. Mechanism of unfaulting of the {113} planar defects

The {113} defects are frequently unfaulted and transformed into perfect dislocation loops of interstitial type on the {113} plane. About the mechanism of the unfaulting of the {113} planar defects, we think that the unfaulting can be explained mainly by the transformation of the sequence of the I units into the perfect crystal containing additional two net {113} atomic layers. This can be performed only by changing the bond topology at the core of the I unit and introducing simultaneous additional rigid-body translation mainly along the ⟨332⟩ direction.

Here, let us discuss the transformation of the sequence of I units containing no O units, and discuss the effect of the O units finally in this section. The necessary additional translation for the unfaulting of the sequence of the I units is estimated as follows. For the structure where the perfect crystal is cut along the {113} plane and the two {113} atomic layers are inserted, one of the necessary minimum rigid-body translations between the two crystals, so as to maintain the crystal perfection, is $a_0[113]/11$ normal to the {113} plane plus $-3a_0[-3,-3,2]/22$ parallel to the {113} plane within the same context of the present definition of the rigid-body translation of the {113} defects. The optimum translation of the $|I|$ model in Table I can be expressed as $0.92a_0[113]/11$ plus $0.35a_0[-3,-3,2]/22$. Thus the necessary additional translation for the unfaulting of the calculated structure of the $|I|$ model is a small dilatation of $0.08a_0[113]/11$ plus a shift of $-3.35a_0[-3,-3,2]/22$ parallel to the {113} plane. Of course, there exist

other types of the necessary minimum translations so as to maintain the crystal perfection when the two {113} atomic layers are inserted, and there might exist other possible crystallographic selections for the necessary additional translation for the unfaulting. However, the present type of additional translation is minimum for the $|I|$ model and related structures.

In the present case, the change of the bond topology of the I unit into the perfect crystal can be easily performed only by rotating the interstitial atom chain around the ⟨110⟩ axis as shown in Fig. 5, under the simultaneous shift of the crystals on both sides of the defect discussed above. This procedure is the transformation from the hexagonal Si layers between the sequence of five- and seven-membered rings into the diamond Si layers.

The present transformation of the planar defect into the perfect crystal causes the dislocations at the edges of the planar defect and results in a perfect dislocation loop. The Burgers vector of such dislocations is $a_0[110]/2$ as examined experimentally,[2] which can be understood by the present discussion as the following equation:

$$a_0[113]/11+3a_0[3,3,-2]/22\rightarrow a_0[110]/2\ . \quad (4)$$

The core structure of such dislocations can be easily explained by the E units in Fig. 1 which constitute the edges of the {113} planar defects. After the neighboring I units are transformed into the perfect crystal as shown in Fig. 5, the five- and seven-membered rings in the E units can remain without changing bond topology, and such structures correspond to the reconstructed core structure of the edge dislocation proposed by Hornstra.[35]

The present mechanism of the unfaulting does not need long-range atomic diffusion, which is consistent with the observed rapid unfaulting.[2] The energy gain in the unfaulting should be determined by the relation between the energy gain by the transformation of the sequence of the I units into the perfect crystal and the energy increase by the accompanied rigid-body translation and the formation of the dislocation loop. This procedure should be dominated by the area of the planar defects. It should be noted that the sequence of the I units contains a high density of the strain energy as shown in the calculated interfacial energies in Tables I and II.

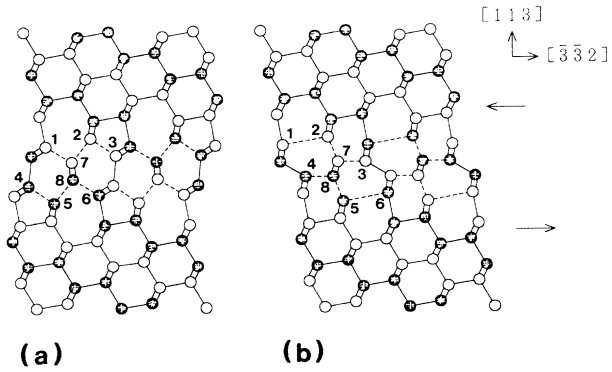

FIG. 5. The mechanism of the unfaulting of the {113} planar defects in Si. The sequence of the I units (a) is transformed into the perfect crystal (b) under the shift of the crystals along the ⟨332⟩ direction. Arrows indicate the directions of the shift. Dashed lines indicate the bonds which are changed through the transformation.

Of course, in the {113} planar defects, the sequence of the I units contains the O units as discussed in Sec. IV E. In the present mechanism, the O unit between the I units should be transformed into a similar unit containing distorted eight-membered rings or a chain of vacancies along the ⟨110⟩ direction, and this part seems to contain larger energy than the O unit without additional absorption of self-interstitials. Thus the total energy gain in the unfaulting should be also influenced by the presence of the O units. It should be possible that the presence of the O units acts so as to stabilize the {113} planar defects in the viewpoint of the prevention against the unfaulting in addition to the viewpoint of the strain energy discussed in Sec. IV E.

V. SUMMARY AND CONCLUSIONS

The atomic structure and energy of the {113} planar interstitial defects in Si have been examined by computer simulations using the Stillinger-Weber potential, based on the atomic model recently proposed by Takeda from the cross-sectional HRTEM image. The atomic model is described by arrangement of the two kinds of structural units on the {113} plane, which consist of atomic rings without any dangling bonds in the ⟨110⟩ projection. One kind of unit is characterized by an eight-membered ring, and another kind of unit contains an interstitial atom chain along the ⟨110⟩ direction, which constitutes a tiny rod of hexagonal Si. The former and latter units are called an O unit and an I unit, respectively, in the present paper. Also it is possible to define structural units constituting the edges of the {113} defects and the perfect crystal. It has been shown that the atomic models where the composition and arrangement of the structural units are similar to the observed structure, such as the $|IO|$, $|IOIIO|$, $|IIO|$, and $|IIIO|$ models, contain relatively small bond-length and bond-angle distortions, of which the range is similar to those in the ⟨110⟩ symmetrical tilt grain boundaries in Si, such as the {221} $\Sigma=9$ boundary. It has been shown that these models have much smaller energies per aggregated interstitial atom than the energy of an isolated self-interstitial in bulk Si. And the calculated optimum rigid-body translations of these models are essentially similar to the observed one. All these results indicate the possible existence of the proposed atomic structure of the {113} planar defects.

Through calculations of various models with various composition or arrangement of the structural units, we have obtained a lot of interesting results that can well explain the observed structure and properties of the {113} planar defects. The results and discussion are summarized as follows.

(1) It has been shown that the eight-membered rings, namely, the O units, can be stabilized by being sandwiched separately between the I units. This is consistent with the HRTEM observations, where the O units are arranged separately between the I units and no O

units neighboring side by side on the {113} plane have been observed. This means that the density of the *O* units does not exceed 50%.

(2) It has been found that the *I* units are more stable in neighboring side by side on the {113} plane as compared with isolated *I* units in the bulk crystal. Thus the mechanism of generation of the {113} planar defects can be explained by the nucleation of the rodlike defects consisting of the *I* units and the growth to the planar defects through sequential generation of the *I* units side by side on the {113} plane.

(3) It has been shown that the *O* units arranged separately in the sequence of the *I* units act so as to relax the strain energy at the sequence of the *I* units. This is the main origin of the observed arrangement of the structural units in the {113} planar defects, where the *O* units are inserted separately at intervals of one or two *I* units, occasionally three *I* units. The reason why the interstitial atoms are aggregated on the {113} plane in Si or Ge is the sequential generation of the *I* units on the {113} plane and the stabilization by introducing the *O* units.

(4) The unfaulting of the {113} defects into the dislocation loops can be explained as the transformation of the sequence of the *I* units into the perfect crystal containing two additional net {113} atomic layers. This can be performed only by changing the bond topology at the core of the *I* units with simultaneous additional rigid-body translation along the ⟨332⟩ direction. It might be possible that the *O* units act so as to prevent the unfaulting.

In conclusion, we have shown that the atomic structure of the {113} planar defects in Si or Ge proposed by Takeda can exist stably and that the atomic structure and the mechanism of generation and unfaulting of the {113} defects can be understood from the viewpoint of the arrangement, energy, generation, and transformation of the structural units without any direct effects of impurities. The structural units in the {113} defects have the ⟨110⟩ rodlike morphology[4] and consist of atomic rings without any dangling bonds as well as those in the ⟨110⟩ symmetrical tilt grain boundaries or dislocations in Si or Ge. This is one of the general features of lattice defects in covalent crystals such as Si or Ge, and is originated from the nature of covalent bonding which demands that all the atoms are four coordinated. It can be said that the peculiar feature of the {113} planar defects in Si or Ge is dominated by the general nature of covalent crystals.

[1]C. A. Ferreira Lima and A. Howie, Philos. Mag. **34**, 1057 (1976).

[2]I. G. Salisbury and M. H. Loretto, Philos. Mag. A **39**, 317 (1979).

[3]A. Bourret, in *Microscopy of Semiconducting Materials,* Proceedings of the Institute of Physics Conference held at Oxford University, 6–8 April 1987, edited by A. G. Cullis and P. D. Augustus, IOP Conf. Proc. No. 87 (Institute of Physics and Physical Society, London, 1987), p. 39.

[4]T. Y. Tan, Philos. Mag. A **44**, 101 (1981).

[5]T. Y. Tan, H. Foell, S. Mader, and W. Krakow, in *Defects in Semiconductors,* edited by J. Narayan and T. Y. Tan (North-Holland, New York, 1981), p. 179.

[6]M. Hirabayashi, K. Hiraga, and D. Shindo, Ultramicroscopy **9**, 197 (1982).

[7]H. Bartsch, D. Hoel, and G. Kastner, Phys. Status Solidi A **83**, 543 (1984).

[8]S. Takeda, Jpn. J. Appl. Phys. **30**, L639 (1991).

[9]S. Takeda, S. Muto, and M. Hirata, Jpn. J. Appl. Phys. **29**, L1698 (1990).

[10]S. Takeda, M. Hirata, S. Muto, Guo-Chun Hua, K. Hiraga, and M. Kiritani, Ultramicroscopy **39**, 180 (1991).

[11]J. Hornstra, Physica **25**, 409 (1959).

[12]A. Bourret and J. J. Bacmann, Surf. Sci. **162**, 495 (1985).

[13]A. Bourret and J. J. Bacmann, Trans. Jpn. Inst. Met. Suppl. **27**, 125 (1986).

[14]R. E. Thomson and D. J. Chadi, Phys. Rev. B **29**, 889 (1984).

[15]D. P. DiVincenzo, O. L. Alerhand, M. Schluter, and J. W. Wilkins, Phys. Rev. Lett. **56**, 1925 (1986).

[16]M. Kohyama, R. Yamamoto, Y. Watanabe, Y. Ebata, and M. Kinoshita, J. Phys. C **21**, L695 (1988).

[17]A. T. Paxton and A. P. Sutton, Acta Metall. **37**, 1693 (1989).

[18]M. Kohyama, S. Kose, M. Kinoshita, and R. Yamamoto, J. Phys. Condens. Matter **2**, 7809 (1990).

[19]F. H. Stillinger and T. A. Weber, Phys. Rev. B **31**, 5262 (1985).

[20]J. Q. Broughton and X. P. Li, Phys. Rev. B **35**, 9120 (1987).

[21]M. D. Kluge, J. R. Ray, and A. Rahman, Phys. Rev. B **36**, 4234 (1987).

[22]I. P. Batra, F. F. Abraham, and S. Ciraci, Phys. Rev. B **35**, 9552 (1987).

[23]A. S. Nandedkar and J. Narayan, Philos. Mag. A **61**, 873 (1990).

[24]S. R. Phillpot and D. Wolf, Philos. Mag. A **60**, 545 (1989).

[25]J. Narayan and A. S. Nandedkar, Philos. Mag. B **63**, 1181 (1991).

[26]B. W. Dodson, Phys. Rev. B **33**, 7361 (1986).

[27]E. Blaisten-Barojas and D. Levesque, Phys. Rev. B **34**, 3910 (1986).

[28]B. P. Feuston, R. K. Kalia, and P. Vashishta, Phys. Rev. B **35**, 6222 (1987).

[29]J. Tersoff, Phys. Rev. B **38**, 9902 (1988).

[30]J. R. Chelikowsky, J. C. Phillips, M. Kamal, and M. Strauss, Phys. Rev. Lett. **62**, 292 (1989).

[31]M. T. Yin and M. L. Cohen, Phys. Rev. B **26**, 5668 (1982).

[32]S. Takeda, S. Muto, and M. Hirata, Mater. Sci. Forum **83-87**, 309 (1992).

[33]R. Car, P. J. Kelly, A. Oshiyama, and S. T. Pantelides, Phys. Rev. Lett. **52**, 1814 (1984).

[34]M. Hasebe, R. Oshima, and F. E. Fujita, Jpn. J. Appl. Phys. **25**, 159 (1986).

[35]J. Hornstra, J. Phys. Chem. Solids **5**, 129 (1958).

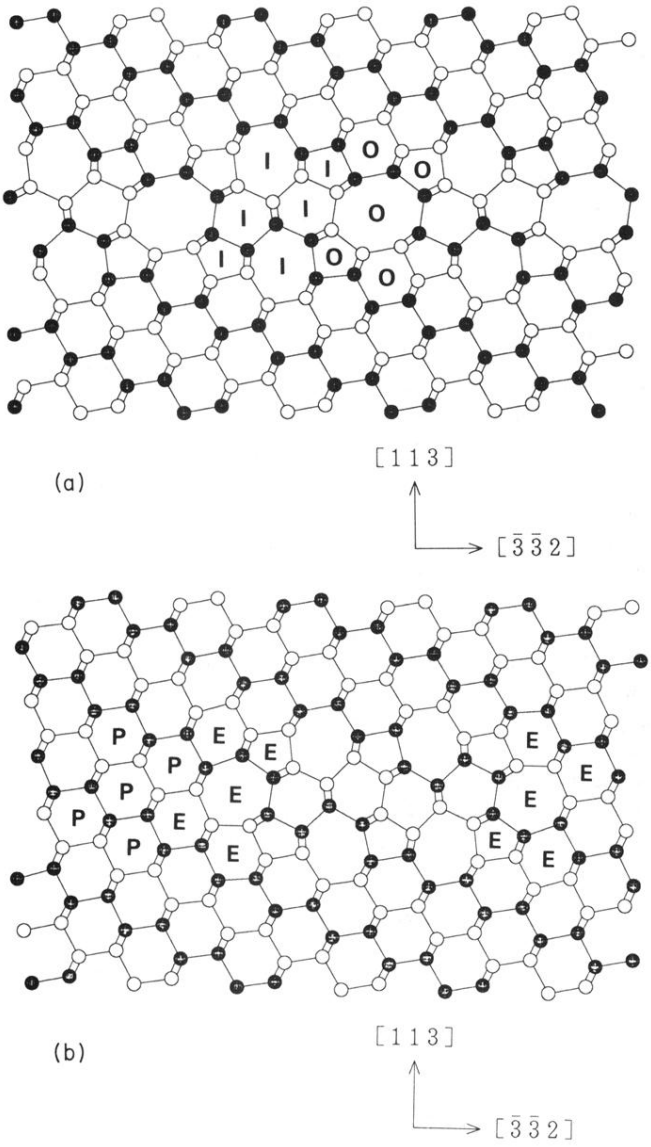

FIG. 1. The ⟨110⟩ projection of the structural units constituting the {113} defects in Si. (a) *I* and *O* units. (b) *E* and *P* units. Atomic rings constituting the respective units are indicated by the symbols of the units. The open and closed circles indicate the atoms of the two different atomic heights along the ⟨110⟩ direction.